Volume 1 | Number 1 | Jan 2013 | Pages 1–100

Journal of
Materials Chemistry C

Materials for optical and electronic devices
www.rsc.org/materialsC

ROYAL SOCIETY
OF CHEMISTRY

ROYAL SOCIETY
OF CHEMISTRY

www.rsc.org/materialsC

ARTICLE TYPE

Crystal Structure Refinement and Luminescence Property of Blue-Green-Emitting CaSrAl$_2$SiO$_7$:Ce^{3+},Li$^+$,Eu^{2+} Phosphors

Shihai Miao[1], Zhiguo Xia[1,2,*], Maxim S. Molokeev[3,4], Jie Zhang[1], Quanlin Liu[2]

Ce^{3+}/Li$^+$, Eu^{2+} singly doped and Ce^{3+}/Li$^+$/Eu^{2+}-co-doped CaSrAl$_2$SiO$_7$ phosphors have been prepared by the conventional solid-state reaction method. The crystal structure of melilite-type CaSrAl$_2$SiO$_7$ phase and the preferred crystallographic positions 10 of the doped ions were refined using Rietveld method. The luminescence properties and energy transfer of CaSrAl$_2$SiO$_7$:Ce^{3+},Li$^+$,Eu^{2+} were studied in detail. Ce^{3+}/Li$^+$ activated CaSrAl$_2$SiO$_7$ phosphor has a strong absorption band in the range of 200-450 nm and perform a blue emission centered at 15 477 nm. When Eu^{2+} ions are co-doped with Ce^{3+}/Li$^+$, the emission color of CaSrAl$_2$SiO$_7$:Ce^{3+},Li$^+$,Eu^{2+} phosphors under the irradiation of 365 nm can be tuned from blue to green via the energy transfer from Ce^{3+} to Eu^{2+} ions. Also the involved energy transfer process and the corresponding mechanism between Ce^{3+} 20 and Eu^{2+} have been discussed in detail. These results indicate that the as-reported CaSrAl$_2$SiO$_7$:Ce^{3+},Li$^+$,Eu^{2+} phosphors have potential applications in near-UV chip pumped white LEDs.

1   Introduction

Silicate-based phosphors have gained enormous academic and 25 commercial interests because of their rigid crystal structure, abundant crystalline phase, multi-color emission and high luminous efficiency, and suitable physical and chemical features.[1-4] Herein, many melilite-based phosphors have been developed as the key materials used in different optical 30 application fields. Zhang reported the tunable bluish green to yellowish green Ca$_{2(1-x)}$Sr$_{2x}$Al$_2$SiO$_7$:Eu^{2+} phosphors.[5] Wu reported the Ce^{3+} and Eu^{2+} codoped Ca$_2$Al$_2$SiO$_7$ phosphor and discussed the photoluminescence and thermoluminescence properties.[6] Li also reported the luminescent properties of 35 Sr$_2$Al$_2$SiO$_7$:Ce^{3+},Eu^{2+} phosphors and discussed the possible application for near UV-excited white light-emitting diodes (*w*-LEDs).[7] Chuai reported the Ca$_2$Al$_2$SiO$_7$:Eu^{3+} phosphor by using the sol-gel method, and they found that the Eu^{3+} emission is markedly dependent of the structural properties of Ca$_2$Al$_2$SiO$_7$.[8] 40 Jiao reported the Ca$_2$Al$_2$SiO$_7$:Ce^{3+},Tb^{3+} phosphor[9] and Simondi reported the Ca$_2$Al$_2$SiO$_7$:Yb^{3+},Er^{3+} phosphor.[10] Pan synthesized the Ce^{3+}/Tb^{3+} codoped Sr$_2$Al$_2$SiO$_7$ phosphors via sol-gel method for *w*-LEDs.[11] Ding reported the long persistent Sr$_2$Al$_2$SiO$_7$:Eu^{2+},Dy^{3+} phosphors.[12] Zou reported a highly thermal 45 stable and waterproof red phosphor Sr$_2$Al$_2$SiO$_7$:Pr^{3+}.[13] However, as for the middle component between the end members of

Sr$_2$Al$_2$SiO$_7$ and Sr$_2$Al$_2$SiO$_7$, viz. CaSrAl$_2$SiO$_7$ phase, there are little report on this type of phosphors except for the investigation on the luminescent properties of SrCaSiAl$_2$O$_7$:Eu^{2+} and 50 CaSrAl$_2$SiO$_7$:Eu^{3+} phosphor.[14-15] But the phase structure is not carefully addressed, and there are no reports about the luminescence properties of Ce^{3+} or Eu^{2+} doped CaSrAl$_2$SiO$_7$ phosphors till now.

Ce^{3+} and Eu^{2+} with broad-band excitation and emission act as 55 two important activators, which have been widely used for luminescent materials for illumination applications, such as *w*-LEDs phosphors. This is mainly ascribed to that their special emission properties combining a broad emission spectrum results in good color rendering properties, short decay times that can 60 avoid saturation. Moreover, the relatively little Stokes shift that allow excitation in the blue or near-UV part of the spectrum will also results in the high luminescence efficiency.[16] The lanthanide ion Ce^{3+} exhibits 4f-5d emission in visible spectral or ultraviolet region and the emission is adjustable depending on the host 65 lattice. In some Eu^{2+} doped matrices, the blue to red emission and blue-light to UV excitation are usually observed through the lower energy of centroid of 5d level and the powerful crystal-field splitting. Consequently, Eu^{2+} can be sensitized by the outstanding blue-emitting Ce^{3+} because of the spectral overlap 70 between excitation band of Eu^{2+} and emission band of Ce^{3+}. So in a Ce^{3+}/Eu^{2+} co-doped single composition host we can expect to achieve adjustable emission spectrum based on the energy transfer between Ce^{3+} and Eu^{2+}.[17,18]

To the best our knowledge, no research has been carried out 75 when CaSrAl$_2$SiO$_7$ was selected as the host doped with Ce^{3+} and Eu^{2+} ions up to now. In the present work, we reported the crystal structure refinement of CaSrAl$_2$SiO$_7$ and preferred crystallographic sites for activators. CaSrAl$_2$SiO$_7$ crystallizes in a tetragonal unit cell with space group *P*-42$_1$*m* and lattice constants 80 of *a* = 7.7595(2) Å, *c* = 5.1680(2) Å, and cell volume = 311.16(2) Å^3 based on the powder diffraction Rietveld refinement. Moreover, we have demonstrated a novel blue-green tunable CaSrAl$_2$SiO$_7$:Ce^{3+},Li$^+$,Eu^{2+} phosphor by varying the relative ratio of Ce^{3+}/Eu^{2+}. Their detailed luminescence properties and the 85 energy transfer between Ce^{3+} and Eu^{2+} have been discussed, and the energy transfer mechanism between Ce^{3+} and Eu^{2+} ions has been investigated systematically.

2   Experimental section

2.1 Materials and synthesis

The designed $Ca_{1-2x}Sr_{1-y}Al_2SiO_7:xCe^{3+},xLi^+,yEu^{2+}$ phosphors were synthesized by conventional high temperature solid-state reaction. The starting materials used were as follows, $SrCO_3$ (A.R.), $CaCO_3$ (A.R.), Li_2CO_3 (A.R.), Al_2O_3 (A.R.), SiO_2 (A.R.), CeO_2 (99.99%), Eu_2O_3 (99.99%). After mixing and grinding in an agate mortar for 20 min, the mixture was placed in a crucible and then sintered at 1300℃ for 5h, in a reducing atmosphere of H_2 (10%) and N_2 (90%) to produce the final samples. Finally, the prepared phosphors were cooled to room temperature and reground for further measurements.

2.2 Characterization

The phase structures of the as-synthesized samples were checked by D8 Advance diffractometer (Bruker Corporation, Germany) operating at 40 kV and 40 mA with Cu Kα radiation (λ = 1.5406 Å). The photoluminescence emission (PL) and photoluminescence excitation (PLE) spectra were carried out by a fluorescence spectrophotometer (F-4600, HITACHI, Japan) equipped with a photomultiplier tube operating at 400 V, and a 150 W Xenon lamp as the excitation source. The luminescence decay curves were obtained using a FLSP9200 fluorescence spectrophotometer (Edinburgh Instruments Ltd., U.K.), and a nF900 flash lamp was used as the excitation resource.

3 Results and discussion

3.1 Phase formation and crystal structure

As we know, the difference of the valence state and ionic radius plays an important role when the possible substitution is considered in the inorganic solid state materials. The ionic radius (IR) of Eu^{2+} (r = 0.125 nm, when coordination number (CN) = 8) is close to that of Sr^{2+} (r = 0.126 nm at CN = 8), while the IR of Ca^{2+} (r = 0.112 nm at CN = 8) is close to that of Ce^{3+} (r = 0.114 nm at CN = 8), but the valence state is different, so that a possible coupled substitution of Ce^{3+}-Li^+ (Li^+: r = 0.092 nm at CN = 8) for two Ca^{2+} can be expected. Based on the above crystal chemistry analysis, we can design the chemical formula as $Ca_{1-2x}Sr_{1-y}Al_2SiO_7:xCe^{3+},xLi^+,yEu^{2+}$, and the real preferred crystallographic positions of the doped ions were refined using Rietveld method, which will be discussed later. Firstly, Fig.1 presents the XRD patterns of as-prepared $Ca_{0.9}SrAl_2SiO_7:0.05Ce^{3+},0.05Li^+$ (i), $Ca_{0.9}Sr_{0.995}Al_2SiO_7: 0.05Ce^{3+},0.05Li^+,0.005Eu^{2+}$ (ii), and the standard data for $CaSrAl_2SiO_7$ (JCPDS 26-327) is also shown as a reference. The two as-prepared samples exhibit the same diffraction peaks, which can be indexed to the phase of $CaSrAl_2SiO_7$ (JCPDS 26-327), and no other phases were detected. Therefore, our samples are of phase purity and the activators of Ce^{3+}/Li^+ and Eu^{2+} ions have dissolved into the crystal lattice of $CaSrAl_2SiO_7$.
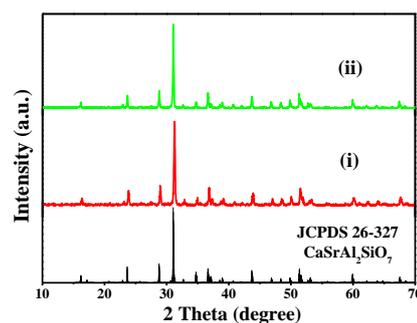
Fig. 1. XRD patterns of $Ca_{0.9}SrAl_2SiO_7:0.05Ce^{3+},0.05Li^+$ (i), $Ca_{0.9}Sr_{0.995}Al_2SiO_7: 0.05Ce^{3+},0.05Li^+,0.005Eu^{2+}$ (ii). The standard data for $CaSrAl_2SiO_7$ (JCPDS 26-327) is shown as a reference.

It is found that no Inorganic Crystal Structure Database (ICSD) file for the $CaSrAl_2SiO_7$ is available. In order to give an insight into the crystallographic sites and the crystal structure of the melilite-type $CaSrAl_2SiO_7$ phase and the doped ions, the selected sample with designed chemical composition of $Ca_{0.98}SrAl_2SiO_7:0.01Ce^{3+},0.01Li^+$ was refined using Rietveld method performed by using TOPAS 4.2. In such a model, sites of Ca ions were occupied by Sr ion with fixed occupation p = 0.5 and by Ce and Li ions with p = 0.05 and p = 0.05, respectively, according to the chemical formula. Fig.2 shows us the Rietveld refinement of the XRD profile of the selected $Ca_{0.98}SrAl_2SiO_7:0.01Ce^{3+},0.01Li^+$, and the crystal structure of $Ca_{0.98}SrAl_2SiO_7:0.01Ce^{3+},0.01Li^+$ with coordination of the cation with oxygen atoms is also demonstrated. As the tetragonal cell (P-42$_1$m) fits very well majority of the peaks, and the crystal structure data of $Ca_2Al_2SiO_7$ was performed as starting model to solve the structure.[19] As we can find from Fig 2a, it shows the Rietveld refinement result of $Ca_{0.98}SrAl_2SiO_7:0.01Ce^{3+},0.01Li^+$, including the observed patterns (black), calculated patterns (red), and difference patterns (gray) and the Bragg reflections of the calculated patterns, and they give the good result on the agreement. The structure refinement was stable and ended with low R-factors shown in Table 1. That's to say, when doping with 0.01 mol Ce^{3+} and 0.01 mol Li^+ in the $CaSrAl_2SiO_7$ host, it gets a single-phase structure, and the $Ca_{0.98}SrAl_2SiO_7:0.01Ce^{3+},0.01Li^+$ crystallizes in a tetragonal unit cell with space group P-42$_1$m and lattice constants of a = 7.7595(2) Å, c = 5.1680(2) Å, and cell volume = 311.16(2) Å^3. The obtained fitted parameters are χ^2 = 1.22, R_P = 6.94%, and R_{WP} = 9.01%. Furthermore, fractional atomic coordinates and isotropic displacement parameters (Å^2) of $Ca_{0.98}SrAl_2SiO_7:0.01Ce^{3+},0.01Li^+$ are also given in Table 2, and the results show that the designed chemical formula and the preferred crystallographic positions of the doped ions are reasonable. Fig 2b shows the crystal structure of $Ca_{0.98}SrAl_2SiO_7:0.01Ce^{3+},0.01Li^+$ with the corresponding coordination of the cation with oxygen atoms. We know that Ca^{2+} and Sr^{2+} have the same coordination environment. Coordination of the cation sites with oxygen presents that the Sr/Ca was coordinated with eight oxygen atoms. In $CaSrAl_2SiO_7$ host, these are two kinds of Al^{3+} sites which are named Al1 and Al2 for easier identification. The Al1 with four oxygen ions constitute the $Al1O_4$ tetrahedron, and Al2 with Si constitute $(Al2Si)O_4$ tetrahedron. In order to give more information on the $Ca_{0.98}SrAl_2SiO_7:0.01Ce^{3+},0.01Li^+$ phosphor, the crystallographic

information file (CIF) is presented in the ESI.
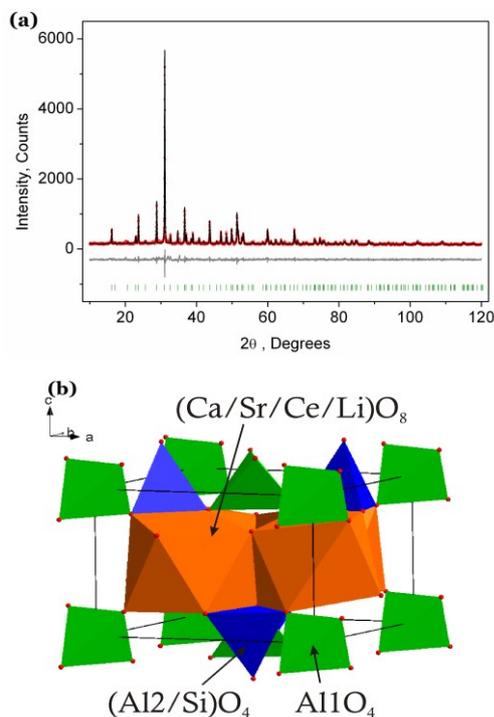
Fig. 2. (a) Rietveld refinement of the XRD profile of Ca$_{0.98}$SrAl$_2$SiO$_7$:0.01Ce^{3+},0.01Li$^+$. (b) Crystal structure of Ca$_{0.98}$SrAl$_2$SiO$_7$:0.01Ce^{3+},0.01Li$^+$ and coordination of the cation with oxygen atoms.

Table 1. Crystallographic data and detail in the data collection and refinement parameters for the Ca$_{0.98}$SrAl$_2$SiO$_7$:0.01Ce^{3+},0.01Li$^+$ sample.

Sp.Gr.	P-42$_1m$
a, Å	7.7595(2)
c, Å	5.1680(2)
V, Å^3	311.16(2)
2θ-interval, °	10-120
Number of reflections	169
Number of refined parameters	32
R_{wp}, %	9.01
R_p, %	6.94
R_{exp}, %	7.40
χ^2	1.22
R_B, %	1.78

Table 2 Fractional atomic coordinates and isotropic displacement parameters (Å^2) of Ca$_{0.98}$SrAl$_2$SiO$_7$:0.01Ce^{3+},0.01Li$^+$.

	x	y	z	B_{iso}	Occ.
Ca	0.3389 (2)	0.1611 (2)	0.5096 (6)	0.83 (7)	0.49
Sr	0.3389 (2)	0.1611 (2)	0.5096 (6)	0.83 (7)	0.5
Ce	0.3389 (2)	0.1611 (2)	0.5096 (6)	0.83 (7)	0.005
Li	0.3389 (2)	0.1611 (2)	0.5096 (6)	0.83 (7)	0.005
Al1	0	0	0	0.4 (3)	1
Al2	0.1404 (4)	0.3596 (4)	0.9631 (10)	0.3 (1)	0.5
Si	0.1404 (4)	0.3596 (4)	0.9631 (10)	0.3 (1)	0.5
O1	0.5	0	0.178 (3)	1.5 (2)	1
O2	0.149 (1)	0.351 (1)	0.279 (2)	1.5 (2)	1
O3	0.0882 (9)	0.1678 (9)	0.812 (2)	1.5 (2)	1

3.2 Luminescent Properties of Ce^{3+}/Li and Eu^{2+} singly or co-doped CaSrAl$_2$SiO$_7$ phosphors

Fig.3a displays the PLE and PL spectra of Ca$_{0.9}$SrAl$_2$SiO$_7$:0.05Ce^{3+},0.05Li$^+$ phosphor. The PLE spectrum monitored at 477nm exhibits a broad band from 250 to 450 nm, which is ascribed to the transitions from the ground state of the Ce^{3+} ions to the field splitting levels of the 5d state.[20] The PL spectrum consists of an asymmetric broad band peaking at 477 nm under the excitation of 365 nm. As we know, such an asymmetric broad band should be ascribed to the characteristics of double-band emission of Ce^{3+}, which is due to the transition of Ce^{3+} ions from the 5d excited state to the ^{2}F$_{7/2}$ and ^{2}F$_{5/2}$ ground states. Fig.3b gives the PL spectra of Ca$_{1-2x}$SrAl$_2$SiO$_7$:xCe^{3+},xLi$^+$ (x = 0.01, 0.03, 0.05, 0.07, 0.10 and 0.15). All the PL spectra exhibited a broad band UV emission centered at 477nm, which was also ascribed to the 5d^1-4f^1 of Ce^{3+} ion. The optimal Ce^{3+} dopant content was found to be 0.05 mol per formula unit and the PL intensity was observed to increase with increasing x when x<0.05. That's to say, with Ce^{3+} dopant content higher than 0.05, concentration quenching was observed and the PL intensity was found to decrease with increasing Ce^{3+}.

(a) Ca$_{0.9}$SrAl$_2$SiO$_7$:0.05Ce^{3+},0.05Li$^+$

λ_{ex} = 365nm
λ_{em} = 477nm

(b) Ca$_{1-2x}$SrAl$_2$SiO$_7$:xCe^{3+},xLi$^+$

x = 0.01
x = 0.03
x = 0.05
x = 0.07
x = 0.10
x = 0.15

λ_{ex} = 365nm
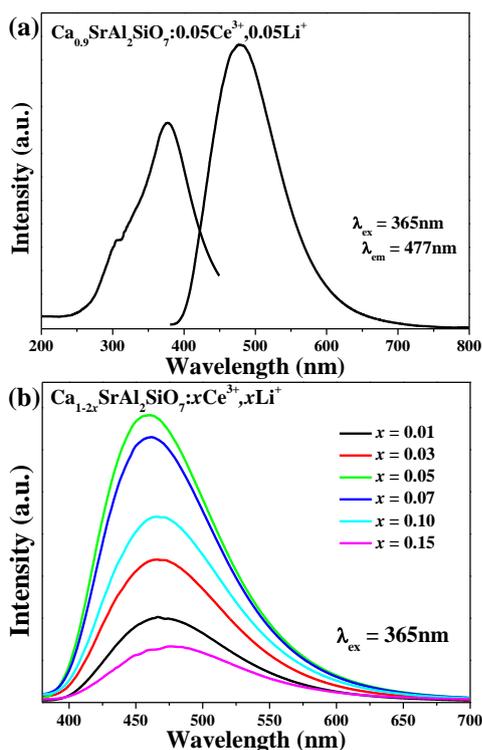
Fig. 3. (a) PLE and PL spectra of Ca$_{0.9}$SrAl$_2$SiO$_7$:0.05Ce^{3+},0.05Li$^+$, (b) PL spectra of Ca$_{1-2x}$SrAl$_2$SiO$_7$:xCe^{3+},xLi$^+$ (x = 0.01, 0.03, 0.05, 0.07, 0.10 and 0.15).

The inset of Fig. 4 shows the PL intensity as a function of Ce^{3+} content for Ca$_{1-2x}$SrAl$_2$SiO$_7$:xCe^{3+},xLi$^+$, and we can clearly find that the optimal doping concentration was determined as x = 0.05 and the intensity declines dramatically as the content of Ce^{3+} exceeds 5 mol % due to the concentration quenching. Furthermore, we can get the intensity of multipolar interaction from the change of the emission intensity which from the emitting level according to the report of Van Uitert. The emission intensity (I) per activator ion follows Eq.:

$$\frac{I}{x} = K\left[1 + \beta(x)^{\theta/3}\right]^{-1} \tag{1}$$

where I is the emission intensity, x is the concentration of the activator ions above the concentration quenching point, β and K are constants for the same conditions, and θ is the function of multipole-multipole interaction for 6 (dipole-dipole), 8 (dipole-quadrupole) or 10 (quadrupole-quadrupole). To obtain a correct θ the dependence of lg(I/x) on lg(x) is plotted, and it yield a straight line with a slope of −θ/3. The fitting result for Ce^{3+} emission centers, which is corresponding to the high Ce^{3+} concentrations Ca$_{1-2x}$SrAl$_2$SiO$_7$:xCe^{3+},xLi$^+$ phosphor compositions, is shown in Fig.4. The slope is -2.990, that the value of θ can be calculated as 8.97, which is approximately equal to 8. It means that the quenching is ascribed to the dipole-quadrupole interaction in the Ca$_{1-2x}$SrAl$_2$SiO$_7$:xCe^{3+},xLi$^+$ phosphor compositions.[21-23]

Slope = -2.990
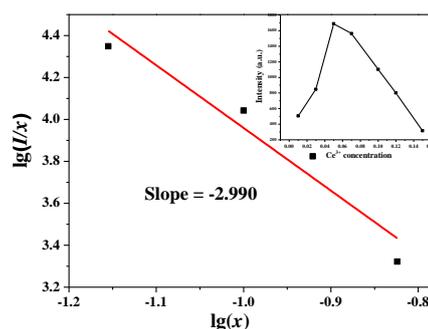
Fig. 4. The relationships of lg(x) versus lg(I/x). The inset shows the PL intensity of the plot of Ca$_{1-2x}$SrAl$_2$SiO$_7$:xCe^{3+},xLi$^+$ as a function of Ce^{3+} content.

Fig.5 presents the emission and excitation spectra of Ce^{3+}/Li$^+$, Eu^{2+} singly doped and Ce^{3+}/Li$^+$/Eu^{2+}-co-doped CaSrAl$_2$SiO$_7$ phosphors. Fig.5a displays the PL and PLE spectra of Ca$_{0.9}$SrAl$_2$SiO$_7$:0.05Ce^{3+},0.05Li$^+$ phosphor. The broad-band emission and excitation behaviors have been discussed above. Fig.5b demonstrates the PL and PLE spectra of CaSr$_{0.995}$Al$_2$SiO$_7$:0.005Eu^{2+}. The PLE spectrum monitored at 542 nm exhibits a broad band from 200 to 500 nm, and the PL spectrum consists of broad band centered at 542 nm under the excitation of 365 nm, which is ascribed to the electric dipole allowed transition of the Eu^{2+} ions. A notable spectral overlap between the PLE spectrum of CaSr$_{0.995}$Al$_2$SiO$_7$:0.005Eu^{2+} and the PL spectrum of Ca$_{0.9}$SrAl$_2$SiO$_7$:0.05Ce^{3+},0.05Li$^+$ is observed. So the energy transfer from Ce^{3+} to Eu^{2+} ions can be achieved in the CaSrAl$_2$SiO$_7$ system.[24] To further confirm the phenomenon, Fig.5c illustrates the PLE and PL spectra Ca$_{0.9}$Sr$_{0.995}$Al$_2$SiO$_7$:0.05Ce^{3+},0.05Li$^+$,0.005Eu^{2+} phosphor. The co-doped phosphor shows a green emission band of Eu^{2+} ions and a blue emission band of Ce^{3+} ions at the irradiation of 365 nm. When monitoring at 542 nm and 477 nm, the peak positions of the PLE spectra are all located at about 365 nm. The above analysis on the PL and PLE spectra of CaSrAl$_2$SiO$_7$:Ce^{3+},Li$^+$,Eu^{2+} phosphors proves the occurrence of the energy transfer from the Ce^{3+} to Eu^{2+} ions.[25]

(a) Ca$_{0.9}$SrAl$_2$SiO$_7$:0.05Ce^{3+},0.05Li$^+$

λ_{ex} = 365nm
λ_{em} = 477nm

(b) CaSr$_{0.995}$Al$_2$SiO$_7$:0.005Eu^{2+}

λ_{ex} = 365nm
λ_{em} = 542nm

(c) Ca$_{0.9}$Sr$_{0.995}$Al$_2$SiO$_7$:0.05Ce^{3+},0.05Li$^+$,0.005Eu^{2+}

λ_{ex} = 365nm
λ_{em} = 477nm
λ_{em} = 542nm
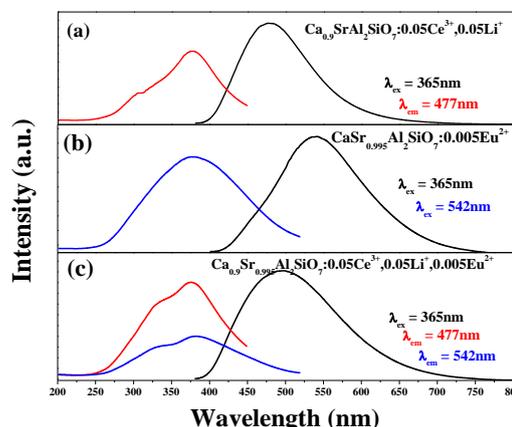
Fig. 5. PLE (left) and PL (right) spectra of Ca$_{0.9}$SrAl$_2$SiO$_7$:0.05Ce^{3+},0.05Li$^+$ (a), CaSr$_{0.995}$Al$_2$SiO$_7$:0.005Eu^{2+} (b), and Ca$_{0.9}$Sr$_{0.995}$Al$_2$SiO$_7$:0.05Ce^{3+},0.05Li$^+$,0.005Eu^{2+} (c).

3.3 Energy Transfer of Ce^{3+}/Li$^+$/Eu^{2+}-co-doped CaSrAl$_2$SiO$_7$ phosphors

As mentioned above, energy transfer can be expected from the spectral overlap of the singly doped samples. Therefore, in order to further investigate the energy transfer process between the Ce^{3+} and Eu^{2+} ions in the $CaSrAl_2SiO_7$ host lattice, we have studied luminescent properties of a series of samples. Fig.6 displays the PL spectra of $Ca_{0.9}Sr_{1-y}Al_2SiO_7:0.05Ce^{3+},0.05Li^+,yEu^{2+}$ samples under 365 nm excitation with a fixed Ce^{3+} content of 0.05 and a varying Eu^{2+} content y in the range of 0-0.010. As shown in Fig.6, we can know that the emission peak has a red shift from 477 nm to 535 nm with the increasing concentration of Eu^{2+}, and the color of phosphors can be tuned from blue to green. The results indicate that energy transfer from Ce^{3+} to Eu^{2+} occurs in $Ca_{0.9}Sr_{1-y}Al_2SiO_7:0.05Ce^{3+},0.05Li^+,yEu^{2+}$ phosphors.
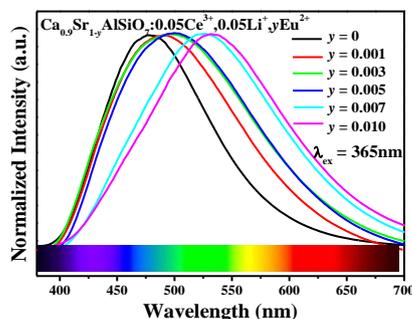
Fig. 6. PL spectra of $Ca_{0.9}Sr_{1-y}Al_2SiO_7:0.05Ce^{3+},0.05Li^+,yEu^{2+}$ (y = 0, 0.001, 0.003, 0.005, 0.007, 0.010) phosphors under 365 nm excitation.

The critical distance R_c among the activators can be calculated by using the following relation:

$$R_c = 2\left(\frac{3V}{4\pi x_c N}\right)^{\frac{1}{3}} \qquad (2)$$

where x_c is the atom fraction of activator at which the quenching occurs; V is the volume of the unit cell and N is the number of $CaSrAl_2SiO_7$ molecular per unit cell. For $CaSrAl_2SiO_7$ host lattice, N = 1, V = 311.16, and x_c is 0.055 denotes the sum of Ce^{3+} concentration of 0.05 and the Eu^{2+} concentration of 0.005. The critical distance R_c is determined to be 22.1Å, which shows that the energy transfer mechanism is governed by multipolar interaction in this system.[26,27]

Under normal circumstances, the energy transfer from the sensitizer to activator maybe a multipolar interaction or via an exchange interaction occurs at higher concentration. According to Dexter's formula of multipolar interaction, the following relation can be obtained:

$$\frac{I_{SO}}{I_S} \propto C^{n/3} \qquad (3)$$

where I_{so} and I_s are the luminescence intensities of Ce^{3+} in the absence and presence of Eu^{2+}, respectively; C is the concentration of the sum of Ce^{3+} and Eu^{2+}; and n = 6, 8, and 10 for dipole–dipole, dipole–quadrupole, and quadrupole–quadrupole interactions, respectively. The relationships between (I_{so}/I_s) vs $C^{n/3}$ are illustrated in Fig.7, and when n = 10 we can observe a linear behavior with the optimum fitting factor of R^2 = 0.9814. The result clearly shows that the energy transfer from Ce^{3+} to Eu^{2+} follows a quadrupole–quadrupole interaction.[28]
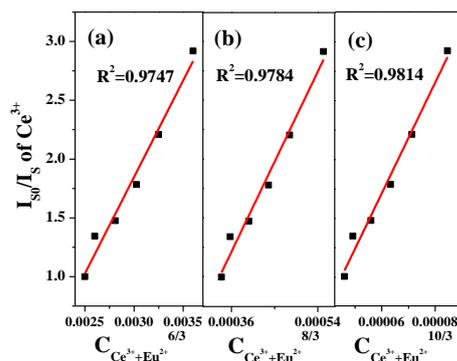
Fig. 7. Dependence of I_{S0}/I_S of Ce^{3+} on (a) $C^{6/3}$, (b) $C^{8/3}$, and (c) $C^{10/3}$.

To further analyze the energy transfer behaviors from Ce^{3+} to Eu^{2+}, lifetime values of Ce^{3+} emission are calculated by analyzing decay curves of $Ca_{0.9}Sr_{1-x}Al_2SiO_7:0.05Ce^{3+},0.05Li^+,xEu^{2+}$ phosphors. Fig.8 gives the fluorescence decay curves of Ce^{3+} emission under excitation at 365 nm and by monitoring emission peak at 477 nm. It is found that all the decay curves can be well fitted with a second-order exponential decay, which can be fitted by the equation:

$$I(t) = I_0 + A_1 \exp(-t/\tau_1) + A_2 \exp(-t/\tau_2) \qquad (4)$$

where $I(t)$ is the luminescence intensity, t is the time, A_1 and A_2 are constants, and τ_1 and τ_2 are rapid and slow decay time for the exponential components, respectively. According to fitting the parameters in Eq. (4), the average lifetime τ^* can be obtained by the formula as follows:

$$\tau^* = (A_1\tau_1^2 + A_2\tau_2^2)/(A_1\tau_1 + A_2\tau_2) \qquad (5)$$

Therefore, the decay lifetime values at 477 nm are determined to be 38.13, 26.97, 23.85, 18.16, 16.65 and 12.01 ns. Obviously the decay lifetime values decreased monotonically as the Eu^{2+} concentration increases, which also strongly demonstrated the energy transfer from Ce^{3+} to Eu^{2+}.
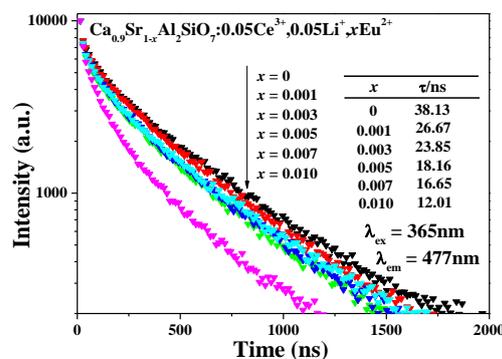
Fig. 8. Decay curves of Ce^{3+} emission in $Ca_{0.9}Sr_{1-x}Al_2SiO_7:0.05Ce^{3+},0.05Li^+,xEu^{2+}$ phosphors under excitation at 365 nm, monitored at 477 nm.

In addition, the energy transfer efficiency η_T between the Ce^{3+} and Eu^{2+} ions can be obtained from the decay lifetime values by using the following equation:[29-30]

$$\eta_T = 1 - \frac{\tau_x}{\tau_0} \qquad (6)$$

where the τ_x and τ_0 represent the lifetime values of sensitizer (Ce^{3+}) ion with and without the presence of activator (Eu^{2+}),

respectively. As shown in Fig.9, the energy transfer efficiencies increase gradually with increasing Eu^{2+} concentration and η_T are calculated to be 0, 30.05, 37.45, 52.37, 56.33 and 68.51% for the $Ca_{0.9}Sr_{1-x}Al_2SiO_7$:$0.05Ce^{3+}$,$0.05Li^+$,$xEu^{2+}$ phosphors with $x = 0$, 0.001, 0.003, 0.005, 0.007 and 0.010, respectively.
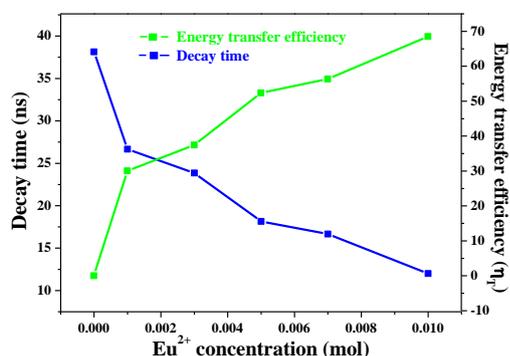
Fig. 9. Dependence of the fluorescence lifetime of the Ce^{3+} and energy transfer efficiency on doped Eu^{2+} molar concentration in $Ca_{0.9}Sr_{1-x}Al_2SiO_7$:$0.05Ce^{3+}$,$0.05Li^+$,$xEu^{2+}$ samples, monitored at 477 nm.
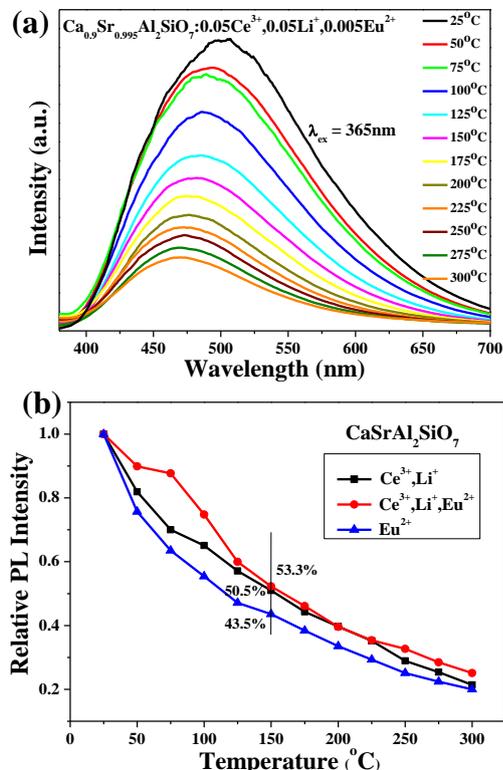
Fig. 10. (a) The PL spectra ($\lambda_{ex} = 365$ nm) of the selected $Ca_{0.9}Sr_{0.995}Al_2SiO_7$:$0.05Ce^{3+}$,$0.05Li^+$,$0.005Eu^{2+}$ phosphor under different temperatures in the range of 25-300 ºC. (b) The relative emission intensities as a function of temperature for typical Ce^{3+}/Li^+, Eu^{2+} singly doped and Ce^{3+}/Li^+/Eu^{2+}-co-doped $CaSrAl_2SiO_7$ phosphors.

3.4 Thermal quenching, CIE chromaticity coordinates and emission colors of $CaSrAl_2SiO_7$:Ce^{3+},Li^+,Eu^{2+}

Thermal quenching behaviors of the selected phosphor have been studied. As shown in Fig. 10a, the temperature dependent emission spectra under the excitation of 365 nm for the selected $Ca_{0.9}Sr_{0.995}Al_2SiO_7$:$0.05Ce^{3+}$,$0.05Li^+$,$0.005Eu^{2+}$ phosphor has been given, and it is found that emission intensities decrease and

the emission peaks shift to the blue region with increasing temperature, which is similar as previous report.[2] Furthermore, the relative emission intensities for the Ce^{3+}/Li^+, Eu^{2+} singly doped and Ce^{3+}/Li^+/Eu^{2+}-co-doped $CaSrAl_2SiO_7$ phosphors as a function of temperature were also given in Fig. 10b. As can be seen, the relative PL intensity slowly decreases with increasing temperature. When the temperature was raised up to 150 ºC, the PL intensity of the sample drops to 53.3%, 50.5% and 43.5% of the initial value at room temperature for the corresponding $Ca_{0.9}SrAl_2SiO_7$:$0.05Ce^{3+}$,$0.05Li^+$, $Ca_{0.9}Sr_{0.995}Al_2SiO_7$:$0.05Ce^{3+}$, $0.05Li^+$,$0.005Eu^{2+}$, and $CaSr_{0.995}Al_2SiO_7$:$0.005Eu^{2+}$ phosphors. It is found that the Ce^{3+}/Li^+/Eu^{2+}-co-doped $CaSrAl_2SiO_7$ phosphor has better thermal stability compared to others.

The CIE chromaticity coordinates for different samples in $Ca_{0.9}Sr_{1-x}Al_2SiO_7$:$0.05Ce^{3+}$,$0.05Li^+$,$xEu^{2+}$ phosphors were measured based on the corresponding PL spectra upon 365 nm excitation, and the results are summarized in Fig.11 and Table 3, respectively. From this diagram, we can see that the emission color of the phosphors can be easily modulated from blue to green by simply change the value of x from 0 to 0.01. Accordingly, the corresponding CIE coordinates of $Ca_{0.9}Sr_{1-x}Al_2SiO_7$:$0.05Ce^{3+}$,$0.05Li^+$,$xEu^{2+}$ change from (0.172, 0.177) to (0.304, 0.408), due to the variation of the emission composition of the Ce^{3+} and Eu^{2+} ions. The inset in Fig.11 also illustrates the digital photos of this series of $Ca_{0.9}Sr_{1-x}Al_2SiO_7$:$0.05Ce^{3+}$,$0.05Li^+$,$xEu^{2+}$ phosphors under 365 nm UV lamp excitation. These results indicate that the $Ca_{0.9}Sr_{1-x}Al_2SiO_7$:$0.05Ce^{3+}$,$0.05Li^+$,$xEu^{2+}$ phosphor may have a broad application prospects for n-UV LEDs.
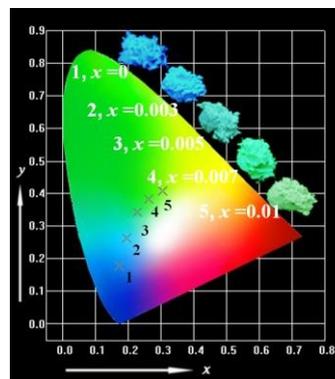
Fig. 11. CIE chromaticity diagram and a series of digital photographs of the selected $Ca_{0.9}Sr_{1-x}Al_2SiO_7$:$0.05Ce^{3+}$,$0.05Li^+$,$xEu^{2+}$ (x = 0, 0.003, 0.005, 0.007, 0.010) phosphors (λ_{ex} = 365 nm).

Table 3 Comparison of the CIE chromaticity coordinates (x, y) for $Ca_{0.9}Sr_{1-x}Al_2SiO_7$:$0.05Ce^{3+}$,$0.05Li^+$,$xEu^{2+}$ (x = 0, 0.003, 0.005, 0.007, 0.010) phosphors excited at 365 nm.

Sample No.	Sample composition (y)	CIE coordinates (x, y)
1	0	(0.172, 0.177)
2	0.001	(0.196, 0.264)
3	0.005	(0.223, 0.344)
4	0.008	(0.262, 0.381)
5	0.015	(0.304, 0.408)

4 Conclusion

In summary, a series of Ce^{3+}/Li^+, Eu^{2+} singly doped and $Ce^{3+}/Li^+/Eu^{2+}$-co-doped $CaSrAl_2SiO_7$ phosphors have been synthesized. Rietveld structure refinement indicates that $CaSrAl_2SiO_7$ crystallizes in a cubic unit cell with space group $P\text{-}42_1m$ and lattice constant of a = 7.76 and c = 5.17. The quadrupole–quadrupole interaction mechanism should be mainly responsible for the energy transfer in $CaSrAl_2SiO_7$:Ce^{3+},Li^+,Eu^{2+} phosphor. The emission color of the obtained phosphors can be tuned from blue (0.172, 0.177) to green (0.304, 0.408) by adjusting the concentration of Eu^{2+}. Energy transfer efficiency between Ce^{3+} and Eu^{2+} increases and when the Eu^{2+} doping content of $x = 0.010$ can get the maximum value of 68.51%. This indicates that $CaSrAl_2SiO_7$:Ce^{3+},Li^+,Eu^{2+} can act as a potential blue-green tunable phosphor for the white light emitting diodes application.

Acknowledgements

Notes and references

[1]*School of Materials Sciences and Technology, China University of Geosciences, Beijing 100083, China*

[2]*School of Materials Sciences and Engineering, University of Science and Technology Beijing, Beijing 100083, China*

[3]*Laboratory of Crystal Physics, Kirensky Institute of Physics, SB RAS, Krasnoyarsk 660036, Russia*

[4]*Department of Physics, Far Eastern State Transport University, Khabarovsk, 680021 Russia*

* E-mail: xiazg@ustb.edu.cn (Z. Xia)

Tel. : +86-10-82377955; Fax. : +86-10-82377955

† Electronic supplementary information (ESI) available: The crystallographic information file (CIF) of $Ca_{0.98}SrAl_2SiO_7$:0.01Ce^{3+},0.01Li$^+$ is given.

Notes and references

1 Z. G. Xia, Y. Y. Zhang, M. Molokeev, V. V. Atuchin and Y. Luo, *Sci. Rep.*, 2013, **3**, 3310.

2 Z. G. Xia, X. M. Wang, Y. X. Wang, L. B. Liao and X. P. Jing, *Inorg. Chem.*, 2011, **50**, 10134-10142.

3 K. A. Denault, J. Brgoch, M. W. Gaultois, A. Mikhailovsky, R. Petry, H. Winkler, S. P. DenBaars and R. Seshadri, *Chem. Mater.*, 2014, **26**, 2275-2282.

4 J. Park, S. J. Lee and Y. J. Kim, *Cryst. Growth Des.*, 2013, **13**, 5204-5210.

5 Q. Zhang, J. Wang, M. Zhang and Q. Su, *Appl. Phys. B*, 2008, **92**, 195-198.

6 H. Y. Wu, Y. H. Hu, G. F. Ju, L. Chen, X. J. Wang and Z. F. Yang, *J. Lumin.*, 2011, **131**, 2441-2445.

7 G. H. Li, M. M. Li, L. L. Li, H. Yu, H. F. Zou, L. C. Zou, S. C. Gan and X. C. Xu, *Mater. Lett.*, 2011, **65**, 3418-3420.

8 X. H. Chuai, H. J. Zhang, F. S. Li and K. C. Chou, *Opt. Mater.*, 2004, **25**, 301-305.

9 H. Y. Jiao and Y. H. Wang, *J. Electrochem. Soc.*, 2009, **156**, 117-120.

10 T. B. Simondi, B. Viana, D. Vivien and A. M. Lejus, *Opt. Mater.*, 1996, **6**, 267-274.

11 W. Pan, G. L. Ning, Y. Lin and X. F. Yang, *J. Rare. Earth.*, 2008, **26**, 207-210.

12 Y. L. Ding, Y. X. Zhang, Z. Y. Wang, W. Li, D. L. Mao, H. B. Han and C. K. Chang, *J. Lumin.* 2009, **129**, 294-299.

13 H. Zou, D. F. Peng, Z. M. Chu, X. S. Wang, Y. X. Li and X. Yao, *J. Mater. Sci.*, 2013, **48**, 7981-7985.

14 C. H. Huang, Y. T. Lai, T. S. Chan, Y. T. Yeh and W. R. Liu, *RSC Adv.*, 2014, **4**, 7811-7817.

15 H. Y. Jiao and Y. H. Wang, *Phys. B*, 2012, **407**, 2729-2733.

16 S. J. Gwak, P. Arunkumar and W. B. Im, *J. Phys. Chem. C*, 2014, **118**, 2686-2692.

17 W. B. Park, S. P. Singh and K. S. Sohn, *J. Am. Chem. Soc.*, 2014, **136**, 2363-2373.

18 S. H. Devon Moore, L. Deakin, M. J. Ferguson and A. Mar, *Chem. Mater.*, 2002, **14**, 4867-4873.

19 M. Merlini, M. Gemmi, G. Cruciani and G. Artioli, *Phys. Chem. Miner.*, 2008, **35**, 147-155.

20 H. K. Park, J. H. Oh, H. Kang, J. Zhang and Y. R. Do, *ACS Appl. Mater. Interfaces.*, 2015, **7**, 4549-4559.

21 C. H. Huang, Y. C. Chiu, Y. T. Yeh, T. S. Chan and T. M. Chen, *ACS Appl. Mater. Interfaces.*, 2012, **4**, 6661-6668.

22 H. Y. Xiao, Z. G. Xia, L. B. Liao, J. Zhou and J. Q. Zhuang, *J. Alloy. Compd.*, 2012, **534**, 97-100.

23 Z. G. Xia, Y. Y. Zhang, M. S. Molokeev and V. V. Atuchin, *J. Phys. Chem. C,* 2013, **117**, 20847-20854.

24 Y. Y. Li, Q. S. Wu, X. C. Wang, J. Y. Ding, Q. Long and Y. H. Wang, *RSC Adv.*, 2014, **4**, 63569-73575.

25 M. M. Shang, G. G. Li, D. L. Geng, D. M. Yang, X. J. Kang, Y. Zhang, H. Z. Lian and J. Lin, *J. Phys. Chem. C*, 2012, **116**, 10222-10231.

26 S. H. Miao, Z. G. Xia, J. Zhang and Q. L. Liu, *Inorg. Chem.*, 2014, **53**, 10386-10393.

27 G. G. Li, D. L. Geng, M. M. Shang, Y. Zhang, C. Peng, Z. Y. Cheng and J. Lin, *J. Phys. Chem. C*, 2011, **115**, 21882-21892.

28 W. Lv, W. Z. Lv, Q. Zhao, M. M. Jiao, B. Q. Shao and H. P. You, *J. Mater. Chem. C*, 2015, **3**, 2334-2340.

29 H. H. Lin, G. B. Zhang, P. A. Tanner and H. B. Liang, *J. Phys. Chem. C*, 2013, **117**, 12769-12777.

30 Z. G. Xia and R. S. Liu, *J. Phys. Chem. C*, 2012, **116**, 15604-15609.

Crystal Structure Refinement and Luminescence Property of Blue-Green-Emitting CaSrAl$_2$SiO$_7$:Ce^{3+},Li^{+},Eu^{2+} Phosphors

Shihai Miao[1], Zhiguo Xia[1,2,*], Maxim S. Molokeev[3,4], Jie Zhang[1], Quanlin Liu[2]

Structure and blue-green tunable luminescence properties of Ce^{3+}/Li^{+}, Eu^{2+} singly doped and Ce^{3+}/Li^{+}/Eu^{2+}-co-doped CaSrAl$_2$SiO$_7$ phosphors have been studied.